Chapter 3

Sensorless control methods of BLDC Motor

Before introducing the sensorless control methods, the detail driver structure of the motor will be shown in section 3.1. The driver structure includes the six-step inverters using PWM signals. The principle of the switching is based on electrical angular position information, which is decoded by three Hall-effect sensors.

In traditional control, the rotor position is detected from the Hall-effect sensors installed inside the motor; however, the rotor position sensors present several drawbacks in many applications when concerning the whole system's cost, size, and reliability. Therefore, resent investigators have paid more and more attentions to sensorless control without any Hall-effect sensors. Many sensorless-related technologies have been proposed, such as back-EMF based position detection and third-harmonics voltage position detection. These methods will be introduced in section 3.2.

Comparing these methods, the method based on the estimator seems to have less constrained and more expansibility. The sliding mode estimator leads to a good robustness of the drive systems to disturbances and uncertain parameters. These ideas are presented in section 3.3.

3.1 The typical driver of BLDC Motor

The model of the 3-phase Y-connected BLDC consists of winding resistances, winding inductances, and back-EMF voltage sources. The inverter circuit and the equivalent model are shown in Figure. 3.1.

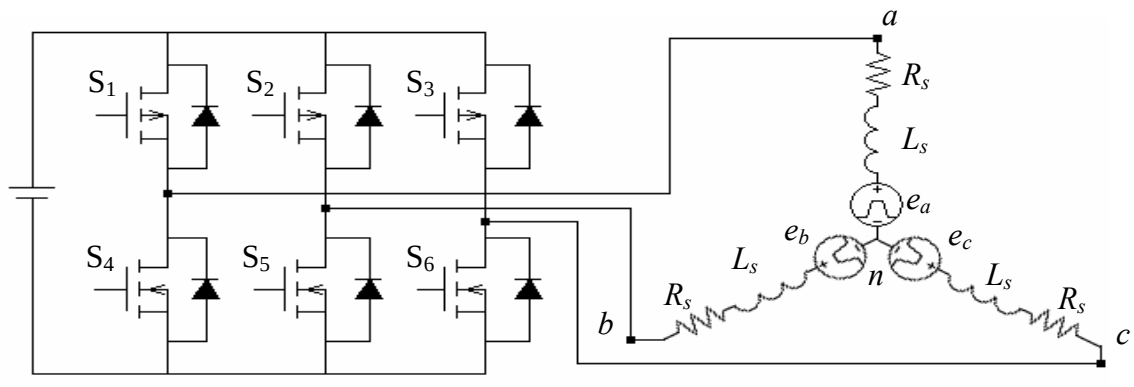

Figure. 3.1 Schematic of the inverter and equivalent modeling for a BLDC motor.

At any angular position in a BLDC motor, only two of the three-phase stator windings are excited by properly switching the inverter to produce a current with a rectangular shape. The inverter circuit of single-phase is cascaded by two power transistors, such as MOSFETs or IGBTs, as the active elements. Both of them can not conduct at the same time to avoid burning under over-current. For example, when the S_1 turns ON, the S_4 must turn OFF. Generally, NMOSFETs are selected to be the power transistors for small power motors. Based on the devices characteristics, to turn ON the NMOSFETs, a high gate voltage should be applied. On the contrary, to turn OFF the NMOSFETs, a low gate voltage should be applied. Therefore, under this control method, the six segments of the stator excitation over a fundamental cycle is

defined and each segment lasts for a period of $\pi/3$, as given in Table. 3.1. In addition, the six segments are processed in order, such as $A\overline{B} \to A\overline{C} \to B\overline{C} \to B\overline{A} \to C\overline{A} \to C\overline{B}$, which can be implemented by the six-step drive, presented in Figure. 3.2.

Table. 3.1 Position based of six segments.

Electrical angle	segment	Switch on
$0^o \sim 60^o$	$A\overline{C}$	S_1, S_6
$60^o \sim 120^o$	$B\overline{C}$	S_2, S_6
$120^o \sim 180^o$	$B\overline{A}$	S_1, S_4
$180^o \sim 240^o$	$C\overline{A}$	S_3, S_4
$240^o \sim 360^o$	$C\overline{B}$	S_3, S_5
$360^o \sim 0^o$	$A\overline{B}$	S_1, S_5

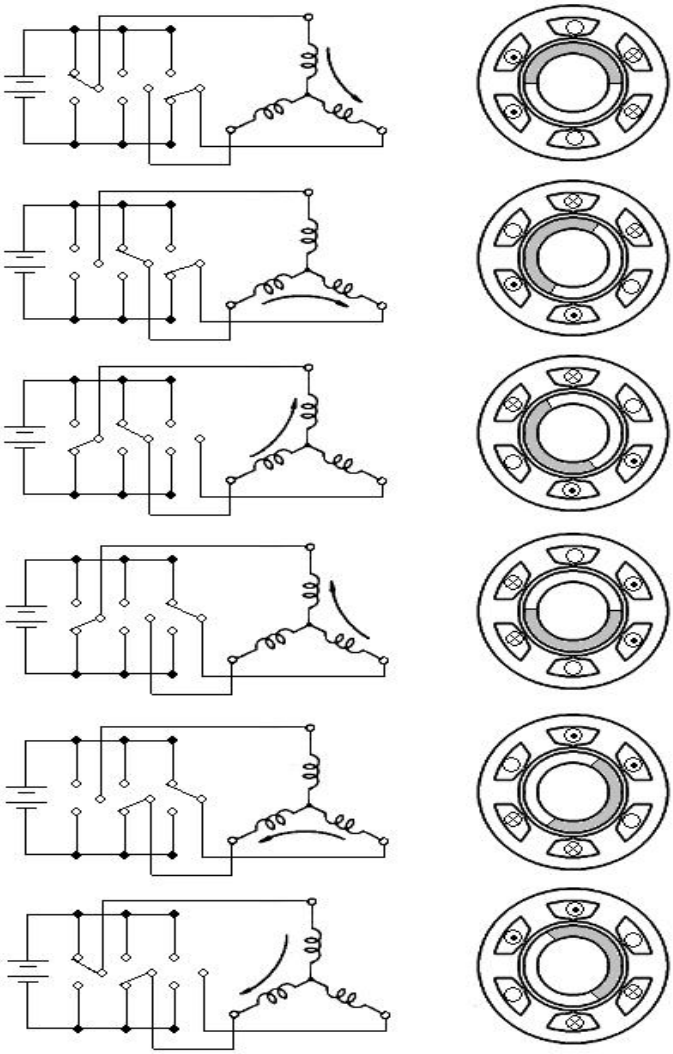

Figure. 3.2 The procedure of the six-step drive.

Typically, the switching communication is based on the rotor position which is measured by three Hall-effect sensors located in the motor. The three Hall-effect sensors can produce digital signals that are in three bits, eight combinations of which will be measured according to the direction of the magnetic field. In practically, each pole will only own two of the three Hall-effect sensors so that “000” and “111” will be eliminated. Therefore, the other six combinations in a circle are thus divided into

six parts, as shown in Figure.3.3. In addition, the tree Hall-effect sensors will share π in electrical angle. In the traditional control experiment, it is easy to know the rotor position and velocity because it just decodes the digital signals from Hall-effect sensors and differential the variance of one digital signal.

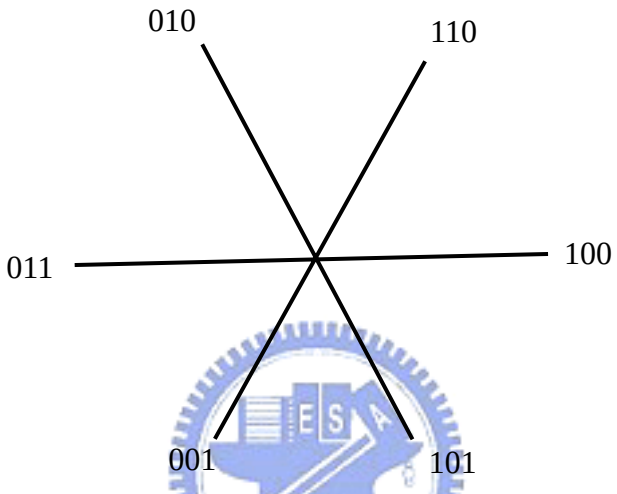

Figure. 3.3 Hall-effect sensors signals of position distribution.

3.2 Review of sensorless control methods for BLDC Motor

For BLDC motors, only the knowledge of six communication instants per electrical is needed. In order to reduce cost and motor size, such sensors may be neglected and position may be estimated. Furthermore, the sensorless control is the only way for some applications and many methods via sensorless control have been researched. The main strategies are back-EMF based position estimation [13], third-harmonics voltage based position estimation [14].

3.2.1 Back-EMF based position estimation method

As the description before, only two of three stator windings are excited at the same time, ant the third stator winding is open during the transition periods between the positive and negative flat segments of the back-EMF. This arrangement provides a chance to sense the back-EMF, and it rotates among the three phase windings when the phase winding excites from one to another. Therefore, each of the motor terminal voltages contains the back-EMF information that can be used to derive the communication instants. The zero-crossing method is employed to determine the switching sequence by detecting the instant where the back-EMF in the unexcited phase crosses zero. Generally, with Y-connected stator windings, three terminals voltages v_{as}, v_{bs} and v_{cs} can be derived as

$$v_{as} = v_{an} + v_n = R_s i_{as} + L_s \frac{di_{as}}{dt} + e_a + v_n \tag{3-1}$$

$$v_{bs} = v_{bn} + v_n = R_s i_{bs} + L_s \frac{di_{bs}}{dt} + e_b + v_n \tag{3-2}$$

$$v_{cs} = v_{cn} + v_n = R_s i_{cs} + L_s \frac{di_{cs}}{dt} + e_c + v_n \tag{3-3}$$

where v_n is the neural voltage, v_{an}, v_{bn} and v_{cn} are the phase voltages with respect to the negative DC bus, i_{as}, i_{bs} and i_{cs} represent the phase currents, and e_a, e_b and e_c are the back-EMF voltages generated in the three unexcited phases. Let S_1 and S_5 turn ON, the terminal voltage v_{as} is equal to V_{DC}, v_{bs} is equal to zero, and v_{cs} is equal to $e_c + v_n$. Suppose that the current applied to the winding is rectangular-shaped and the

inductance voltage drop is negligible, the line-to-line current i_{abs} can be shown as

$$i_{abs} = i_{as} = -i_{bs} = \frac{V_{dc} - (e_a - e_b)}{2R_s} \tag{3-4}$$

Substituting for (3-3), the terminal voltage of phase *c* can be derived as

$$v_c = e_c + v_n = e_c + \frac{V_{dc} - e_a - e_b}{2} \tag{3-5}$$

Since the difference of $2\pi/3$ electrical degree in back-EMF voltage exists between any two phases, there is an instant that $e_c = 0$ and $e_a = -e_b$. Then

$$v_c = v_n = \frac{V_{dc}}{2} \tag{3-6}$$

Hence, the zero-crossing position of e_c is independent of the load current. The prove process is the same when phase *a* or *b* is unexcited. Detecting the zero-crossing instants of the integrator output generates the required phase communication timing signals. The method can be realized by using voltage sensors and low pass filters. However, the modulation noise is eliminated by using the low pass filters which is produced a phase delay varies with the frequency of the excited signal for the desired speed. Besides, the back-EMF voltage is zero at standstill and it is proposed to the rotor speed. This method is difficult to realize at startup or very slow situation.

3.2.2 Third-harmonics voltage based position estimation method

This method is based on the fact that in a symmetrical three phases Y-connected

motor with trapezoidal back-EMF. The six step inverters switches the stator excitation at every $\pi/3$ electrical degree. The switching can be detected by monitoring the third-harmonic voltage of the back-EMF. The stator voltage equation for phase *a*, for instance, is written as

$$v_{as} = R_s i_{as} + L_s \frac{d}{dt}(i_{as}) + e_{as} \tag{3-7}$$

Similar expressions can be written for the other two stator phases. The phase stator resistance inductance are represented as R_s and L_s respectively. The term e_{as} represents the back-EMF voltage. For a full pitch magnet and full pitch stator phase winding, the back-EMF voltages contains the following frequency components

$$e_{as} = E(\cos\omega_e t + k_3 \cos 3\omega_e t + k_5 \cos 5\omega_e t + k_7 \cos 7\omega_e t + ...) \tag{3-8}$$

$$e_{bs} = E(\cos(\omega_e t - 2\pi/3) + k_3 \cos 3(\omega_e t - 2\pi/3) + ...) \tag{3-9}$$

$$e_{cs} = E(\cos(\omega_e t + 2\pi/3) + k_3 \cos 3(\omega_e t + 2\pi/3) + ...) \tag{3-10}$$

Because of Y-connected stator windings, the third-harmonic voltage component at the terminal voltage is only due to the back-EMF. The summation of the three stator phase voltages is a zero sequence which contains a dominant third-harmonic component and high frequency components, expressed as

$$v_{an} + v_{bn} + v_{cn} = 3Ek_3 \cos 3\omega_e t + v_{high\_freq} = v_3 + v_{high\_freq} \tag{3-11}$$

where v_3 is the third-harmonic voltage and v_{high_freq} is the high frequency components. Therefore, the rotor flux can be estimated from this third-harmonic signal by

integrating the resultant voltage v_3,

$$\lambda_{r3} = \int v_3 dt \tag{3-12}$$

In order to obtain the maximum torque per current, the stator current is kept at $\pi/2$ electrical degrees with respect to the rotor flux. It should be notice that the zero crossing of the rotor flux third-harmonic component occur at $\pi/3$ electrical degrees, which are exactly at every desired current communication instant. Thus, detection of the positive zero-crossing of the phase *a* is necessary in order to implement a control algorithm that will command the correct stator currents. From Figure. 3.4, the back-EMF e_{as} is detected, it is clearly that the zero-crossing of the $\lambda_{\gamma 3}$ is the communication instant.

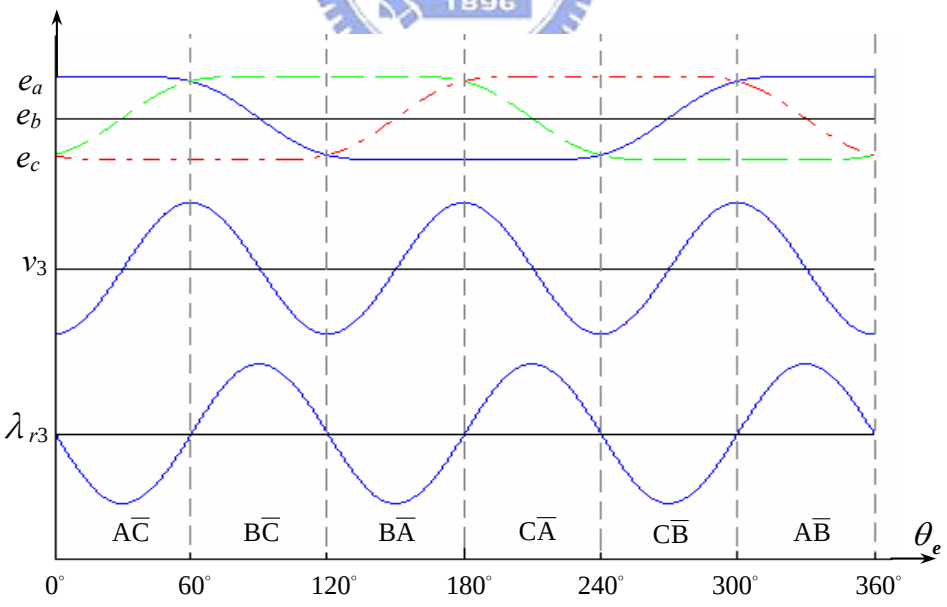

Figure. 3.4 The back-EMF, third-harmonic, and third-harmonic rotor flux of the phase *a* based on the rotor position in electrical degree.

The result of the summation of the three phase voltages contain the

third-harmonic voltage and high frequency sequence components that can be easily eliminated by a low pass filter.

The important advantages of this method are simplicity of implementation, low susceptibility to electrical noise and robustness. On the other hand, this method has good performance at low speed when comparing to the back-EMF based method. But it is difficult to sense the neutral point voltage. So, the neutral terminal is not available due to the cost and structure constrains in application.

3.3 Sliding mode estimator for BLDC Motor's Angular Velocity

The sensorless control method is employed not only to reduce the cost and motor size, but also to avoid the use of Hall-effect sensors, which are sensitive to the motor temperature inside. Two sensorless control methods have been presented before estimate the motor's electrical angle by detecting back-EMFs. Then, the motor's electrical velocity will derive from first derivation. However, they are hard to measure the back-EMFs at start-up or slow rotating velocity. To improve the drawbacks, an estimator for motor's electrical angular velocity will be developed based on sliding mode theory; then the motor's electrical angle is calculated using an integer. Unfortunately, it will have a serious phase lag comparing with actual one. Therefore,

the position estimator will be design simultaneously. This thesis will focus on the estimation of the motor's angular velocity and the detail design process of the estimator for the BLDC motor's angular velocity will be presented in the following.

To control a BLDC motor sensorlessly, an estimator will be required to estimate the motor's electrical angular velocity in stationary reference frame

$$\frac{d}{dt}i_\alpha = -\frac{R}{L}i_\alpha + \frac{1}{L}v_\alpha - \frac{1}{L}E_\alpha \tag{3-13}$$

$$\frac{d}{dt}i_\beta = -\frac{R}{L}i_\beta + \frac{1}{L}v_\beta - \frac{1}{L}E_\beta \tag{3-14}$$

as shown in Chapter 2. Note that all the variables are measurable except the back-EMFs E_α and E_β; thus, the rotor position θ_e is also immeasurable since $\theta_e = -tan^{-1}\left(\frac{E_\alpha}{E_\beta}\right)$.

There are four steps to obtain the electrical angular velocity. First, the sliding mode estimator for angular velocity should be designed. Next, the back-EMFs are estimated by equivalent control theorem, followed by designing another estimator for back-EMFs to estimate the electrical angular velocity. Finally, the estimated electrical angular velocity equals to actual one, which is illustrated by Lyapunov function. From now on, the detail implement will be introduced as follows.

The first step is to design a sliding mode estimator for angular velocity:

$$\frac{d}{dt}\hat{i}_\alpha = -\frac{R}{L}\hat{i}_\alpha + \frac{1}{L}v_\alpha - \frac{1}{L}u_\alpha \tag{3-15}$$

$$\frac{d}{dt}\hat{i}_\beta = -\frac{R}{L}\hat{i}_\beta + \frac{1}{L}v_\beta - \frac{1}{L}u_\beta \tag{3-16}$$

where $u_\alpha = l_1 sign\left(i_\alpha - \hat{i}_\alpha\right)$ and $u_\beta = l_1 sign\left(i_\beta - \hat{i}_\beta\right)$ are estimator inputs and l_1 is a positive constant sliding estimator gain. It is assumed that the parameters R and L are known and identical to those in the model. Subtracting the above equations from the model equations yields the mismatch dynamics

$$\frac{d}{dt}\tilde{i}_\alpha = -\frac{R}{L}\tilde{i}_\alpha - \frac{1}{L}E_\alpha + \frac{1}{L}u_\alpha \tag{3-17}$$

$$\frac{d}{dt}\tilde{i}_\beta = -\frac{R}{L}\tilde{i}_\beta - \frac{1}{L}E_\beta + \frac{1}{L}u_\beta \tag{3-18}$$

where $\tilde{i}_\alpha = i_\alpha - \hat{i}_\alpha$ and $\tilde{i}_\beta = i_\beta - \hat{i}_\beta$ denote the estimator errors.

In the second step, let sliding surface be $s_\alpha = \tilde{i}_\alpha$ and $s_\beta = \tilde{i}_\beta$. According to the equivalent control theorem, the first derivation of the sliding surfaces should be satisfied respectively

$$\dot{s}_\alpha\big|_{u_\alpha = u_{eq\alpha}} = 0 \tag{3-19}$$

$$\dot{s}_\beta\big|_{u_\alpha = u_{eq\beta}} = 0 \tag{3-20}$$

where $u_\alpha\big|_{u_{eq\alpha}} = E_\alpha$ and $u_\beta\big|_{u_{eq\beta}} = E_\beta$ are equivalent control gains. Since the back-EMF terms are bounded, they may be suppressed by discontinuous inputs with $l_1 > max\left(\left|E_\alpha\right|, \left|E_\beta\right|\right)$. Therefore, the sliding surface will appear to zero in finite time. Notice that the equivalent control gains consist of back-EMFs components as $s_\alpha = \tilde{i}_\alpha = 0$ and $s_\beta = \tilde{i}_\beta = 0$. To extract E_α and E_β from the corresponding equivalent control gains, the low pass filters are used.

The third step is to design the estimator for back-EMFs where the motor speed is assumed constant, which implies that $\dot{\omega}_e = 0$. What follows are equations representing the model of the back-EMFs Z_α and Z_β are the low pass filter's outputs.

$$\dot{Z}_\alpha = -\omega_e Z_\beta \tag{3-21}$$

$$\dot{Z}_\beta = \omega_e Z_\alpha \tag{3-22}$$

Let l_2 be a positive constant. Then the estimator for back-EMFs and the estimated velocity could be chosen as

$$\dot{\hat{Z}}_\alpha = -\hat{\omega}_e \hat{Z}_\beta + l_2\left(Z_\alpha - \hat{Z}_\alpha\right) \tag{3-23}$$

$$\dot{\hat{Z}}_\beta = \hat{\omega}_e \hat{Z}_\alpha + l_2\left(Z_\beta - \hat{Z}_\beta\right) \tag{3-24}$$

$$\dot{\hat{\omega}}_e = \left(Z_\alpha - \hat{Z}_\alpha\right)\hat{Z}_\beta - \left(Z_\beta - \hat{Z}_\beta\right)\hat{Z}_\alpha \tag{3-25}$$

If the phase lag from low pass filter is neglected, the Z_α and Z_β are similar to E_α and E_β. Subtracting the above equations from the model equations yields the error equations as follows

$$\dot{\tilde{Z}}_\alpha = -\omega_e Z_\beta + \hat{\omega}_e \hat{Z}_\beta - l_2\left(\tilde{Z}_\alpha\right) \tag{3-26}$$

$$\dot{\tilde{Z}}_\beta = \omega_e Z_\alpha - \hat{\omega}_e \hat{Z}_\alpha - l_2\left(\tilde{Z}_\beta\right) \tag{3-27}$$

$$\dot{\tilde{\omega}}_e = \left(Z_\alpha - \hat{Z}_\alpha\right)\hat{Z}_\beta - \left(Z_\beta - \hat{Z}_\beta\right)\hat{Z}_\alpha \tag{3-28}$$

where $\tilde{Z}_\alpha = Z_\alpha - \hat{Z}_\alpha$, $\tilde{Z}_\beta = Z_\beta - \hat{Z}_\beta$ and $\tilde{\omega}_e = \omega_e - \hat{\omega}_e$ are all estimation errors. When the estimated angular velocity $\hat{\omega}_e$ is substituted for $\omega_e - \tilde{\omega}_e$, a simplified equations are shown as

$$\dot{\tilde{Z}}_\alpha = -\tilde{\omega}_e \hat{Z}_\beta - \omega_e \tilde{Z}_\beta - l_2\left(\tilde{Z}_\alpha\right) \tag{3-29}$$

$$\dot{\tilde{Z}}_\beta = \tilde{\omega}_e \hat{Z}_\alpha + \omega_e \tilde{Z}_\alpha - l_2\left(\tilde{Z}_\beta\right) \tag{3-30}$$

Finally, in order to prove the convergence of the estimator for back-EMFs, a Lyapunov function candidate is chosen as

$$V = \frac{1}{2}\left(\tilde{Z}_\alpha{}^2 + \tilde{Z}_\beta{}^2 + \tilde{\omega}_e{}^2\right) \geq 0 \tag{3-31}$$

The first derivation of the Lyapunov function should always be smaller than zero, as in

$$\dot{V} = -l_2\left(\tilde{Z}_\alpha{}^2 + \tilde{Z}_\beta{}^2\right) \leq 0 \tag{3-32}$$

The value of Lyapunov function will constantly decrease until $\tilde{Z}_\alpha = 0$ and $\tilde{Z}_\beta = 0$. Then substitute $\tilde{Z}_\alpha = 0$ and $\tilde{Z}_\beta = 0$ simultaneously into (3-29) and (3-30). In addition to $\tilde{\omega}_e \hat{Z}_\beta$ and $\tilde{\omega}_e \hat{Z}_\alpha$ terms, the others should be equal to zero so that $\tilde{\omega}_e$ will be zero. At the end of the procedure, the estimated velocity $\hat{\omega}_e$ will be obtained by sliding mode estimator of the back-EMFs.